

# Low Noise Amplifier with 7 K Noise at 1.4 GHz and 25 °C

Sander Weinreb, *Life Fellow, IEEE* and Jun Shi, *Member, IEEE*

**Abstract**— This paper describes a low noise amplifier which is believed will have transformative impact because of the following characteristics: 1) the noise temperature at physical temperature of 25 °C is a factor of 4 lower than typical commercial LNAs, 2) the noise decreases to 4.5 K at a temperature of -40 °C, a temperature realizable with solid-state coolers. 3) the LNA has an integrated, extremely stable noise source to facilitate measurement of system noise temperature, and 4) the amplifier is powered by a DC voltage and controlled by a tone signal on the RF output cable thus requiring no additional wiring. The amplifier benefits systems in the low microwave frequency range with low background temperature, such as those for space communications and radio astronomy, but without the capital and maintenance costs of cryogenic systems. The paper describes the construction and test results with an emphasis on the manufacturability and accuracy of the noise measurements. Finally, the noise of a system deploying the LNA is described.

**Index Terms**— LNA, low noise amplifier, smart LNA, noise temperature.

## I. INTRODUCTION

**T**he topic of this paper is a low noise amplifier operating at ambient temperatures with an exceptional noise temperature of 7 K at 1.4 GHz. This is much lower noise temperature than that available in commercial LNAs as discussed in section VI and is not just the minimum noise temperature of a transistor driven by an optimum generator but is the measured noise temperature at the 50  $\Omega$  input connector of a rugged weatherproof enclosure. The amplifier performance exceeds that of early cryogenic amplifiers introduced by one of the authors 40 years ago [1] and with solid state cooling to -40 °C has comparable noise to more recent cryogenic amplifiers [2] at frequencies below 2 GHz. The development was motivated and supported in part by work on DSA110, a 110  $\times$  4.6 m array for detection and location of fast radio bursts (FRBs), currently one of the hottest topics in astronomy.

The rationale for the exceptional noise is a superb InP HEMT transistor [3] coupled to an extremely low loss input matching network to be described in Section II. Most LNAs in this frequency range utilize GaAs or SiGe transistors in surface mount MMIC packages with a microstrip input network. Our LNA instead utilizes an InP transistor die, wire bonded to a relatively large, high-impedance, suspended-substrate input

transmission line. The typical loss of the input network and transistor package of previous LNAs in the low microwave frequency range is greater than 0.3 dB from the input connector to transistor gate. This adds 21 K to the noise temperature of the intrinsic transistor and explains why commercial LNAs have greater than 30 K noise even with very good transistors. An exception is the 2016 paper by Schlee, et. al. [4] describing a 0.35 to 1.05 GHz LNA with 10 K noise.

The most important, unexpected finding of our work is that the measured noise temperature decreases from 7.4 K to 4.5 K, a factor of 1.64 when the absolute temperature is decreased from 313 K to 233 K, a factor of 1.34, an effect that is contrary to thermal noise which produces noise temperature proportional to physical temperature. This was first observed over 20 years ago by Murti, et al [5] which showed, a 1.92 reduction in minimum noise temperature for a 1.5 reduction of absolute temperature. from 300 K to 200 K. However, this finding was ignored and most subsequent very low noise LNA papers concentrated on noise at cryogenic temperatures. Our careful measurements show the same effect, which has not been explained to date but is a topic of current research, e.g. [6], [7], which is beyond the scope of the applied experimental work presented here. However, in Section III we show that a circuit analysis using the well-established Pospieszalski model [8], [9] replicates the measurement results when the hot-electron noise [10] is adjusted.

The amplifier has application in receiving systems where the background noise temperature,  $T_b$ , is low, of the order of 10 K, as is the case when the LNA is connected to a low-loss antenna with beam pointed at the cold sky [2]. This occurs for satellite communications and radio astronomy but not for terrestrial communications where  $T_b \sim 300$  K. In the low background case, for high performance systems utilizing large and expensive antennas, cryogenic LNAs with noise temperatures <10 K are currently utilized. This increases system cost dramatically ( $\sim$  \$100K) mostly for the cryogenics, which also has high operating cost for power and maintenance. The LNA we describe in this paper is thus a low-cost solution for these applications and enables arrays with multiple feeds on a large reflector or arrays of large numbers of small antennas. The cost per unit area of large antennas increases with antenna diameter and thus, for a given required total area or gain, large arrays of small antennas have less total cost if the receiver cost is small. Thus, the ambient LNA we describe decreases the optimum

Manuscript received June 3, 2020; accepted Nov 5, 2020.

S. Weinreb ([sweinreb@caltech.edu](mailto:sweinreb@caltech.edu)) and J. Shi ([shijun@caltech.edu](mailto:shijun@caltech.edu)), joint first authors, are with California Institute of Technology, Pasadena, CA, 91125

This work was funded in part the U.S. National Science Foundation under Grant NSF.1836018

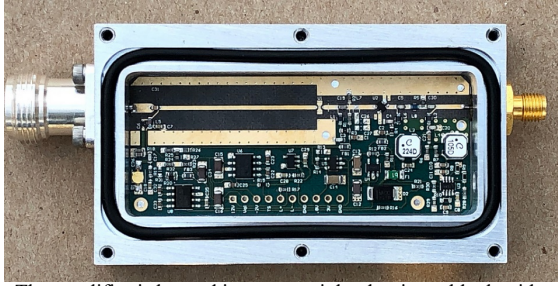


Fig. 1. The amplifier is housed in a water-tight aluminum block with exterior dimensions of  $86 \times 54 \times 22$  mm.

array element size for a minimum total cost and can greatly reduce the cost of large collecting area systems. A future advancement of this principle is the proposed DSA2000, a 2000 element  $\times$  5 m diameter dish array [12], with a wider frequency range, 0.7 to 2 GHz, which may utilize micro-cooling of the input transistor to take advantage of the decreased noise at 233 K.

In section IV the performance of the amplifier installed in the DSA110 radio telescope array is described both to show the LNA noise is low compared to other noises in the system and also to give additional confidence to the noise measured in a very different manner, with the Y factor determined by an absorber at ambient temperature and divided by the cold sky background temperature.

## II. DESCRIPTION

A photograph of the amplifier with cover removed is shown in Fig. 1. The construction is a compromise between requirements for:

- 1) Extremely low loss input matching network and input connector. The losses need to be a fraction of 0.1 dB which would contribute 7 K to the noise. This is realized by a suspended substrate high impedance line on Rogers 5880 material in a 1 cm-square outer conductor cross-section. To reduce input connector loss, a special silver-plated type N connector with a raised boss around the dielectric is utilized to reduce outer conductor contact resistance.
- 2) Ease of manufacture including wire bonding to the input transistor with small pads. Access to many surface mount components is also required for testing and maintenance.
- 3) DC isolation of the input transistor gate to allow biasing and protection. An internal noise calibration signal must also be injected with very low loss.
- 4) Environmental protection as the LNA will be typically used outdoors with a direct connection to an antenna feed. The initial approach was a split block design to allow easy access to the bond wires connecting the input transistor die to the printed-circuit board (PCB). However, this was abandoned due to difficulty of environmental sealing between the three chassis parts. The deep-chassis approach shown in Fig. 1 has been implemented with the wire-bonding performed prior to epoxy bonding of the PCB within the chassis. This allows O-ring seals between the chassis and a flat cover and, also, between connectors and the chassis.

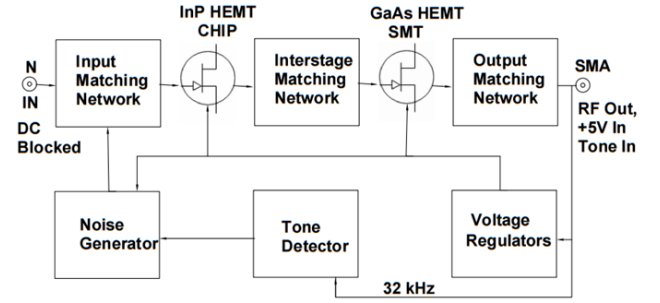


Fig. 2. LNA block diagram. The input matching network is a suspended-substrate line while inter-stage networks are microstrip.

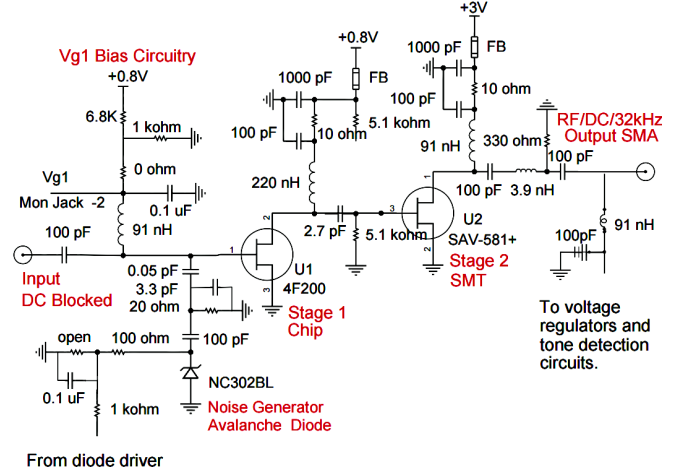


Fig. 3. Schematic of the RF portion of the LNA. Bias settings for stage 1 are:  $V_{ds}$ ,  $I_{ds}$ , and  $V_{gs}$ , are: 0.6 V, 20 mA, and +0.1 V, and for stage 2 are: 2.5 V, 30 mA, and +0.4 V.  $I_{gs}$  and  $I_{gd}$  magnitudes for stage 1 are both less than 0.001  $\mu$ A. The LNA module draws 58 mA at +4 to +6 V with internal calibration off and 82mA with it on.

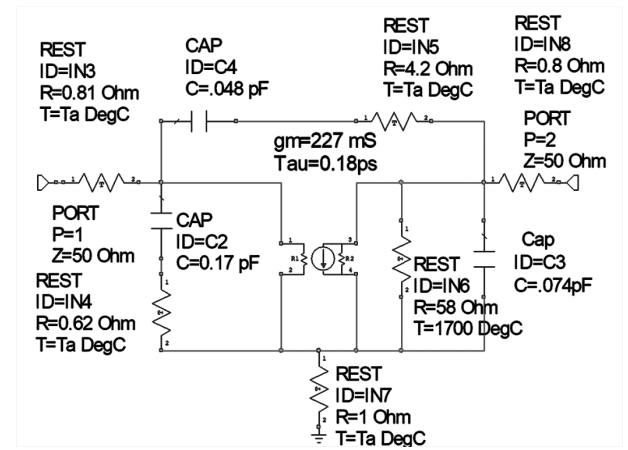


Fig. 4. Small signal and noise model of the first stage transistor appropriate for LNA design below 5 GHz. Omitted are all capacitors  $<0.01$  pF, inductors  $<0.1$  nH, and resistors  $<0.1$   $\Omega$ . Gate leakage is  $<0.001$   $\mu$ A and generates negligible noise. The model is scaled from the  $4 \times 62.5$  model [1] with values slightly changed after wafer probe measurements at Caltech.

A block diagram of the LNA is shown in Fig. 2 with a simplified schematic in Fig. 3, and the model of the first stage Diamics InP high-electron-mobility c transistor [3] in Fig. 4.

The circuit passive elements were determined by manual optimization of the circuit using the AWR circuit simulator using criteria of noise and  $S_{11}$  for the input and interstage

network and  $S_{21}$  and  $S_{22}$  for the output network. The key component is a 45 mm long input transmission line with 155  $\Omega$  impedance. The second stage is a Mini-circuits SAV-581 surface mount transistor.

A unique feature of the LNA is the internal noise calibration source. Most high-performance receiving systems include a noise calibration source based upon a noise diode and directional coupler inserted between the antenna feed and LNA. However, the ambient temperature insertion of these components would contribute too much loss and noise (typically 0.2 dB and 14 K), so a very low loss internal calibration source is included. The initial implementation of this source was with a terminated transistor but this had too much variation with temperature and a surface mount avalanche diode noise source was then utilized. This source has been temperature compensated and will be subject of another publication. The noise is best modeled as a current source injected into the LNA-to-feed connection and thus the noise temperature is dependent upon the impedance of the feed. The injected temperature can be measured in the lab with a 50  $\Omega$  source, but the most relevant value needs to be determined with the LNA connected to the feed. This is accomplished by comparison of the internal calibration noise temperature to that determined by the hot vs sky Y factor realized as absorber material covering the feed aperture compared with cold sky. The internal calibration signal can then be utilized to easily determine the time variation of the system noise temperature,  $T_{\text{sys}}$ .

### III. MEASURED AND MODELED PERFORMANCE

The LNA module  $S$  parameters and noise were measured in an Espec SU-241 bench-top temperature-controlled chamber with forced air controlled at set points from -40  $^{\circ}\text{C}$  to +40  $^{\circ}\text{C}$ . In addition, a thermocouple sensor was attached to the module and indicated a temperature with 2  $^{\circ}\text{C}$  of the air temperature. The measured  $S_{21}$  and  $S_{11}$  magnitudes vs frequency at three different temperatures are shown in Fig. 5. The stability of the gain and input match vs temperature are remarkable with less than 1 dB gain variation from -40  $^{\circ}\text{C}$  to +40  $^{\circ}\text{C}$ ; a coefficient of -0.012 dB/ $^{\circ}\text{C}$ . This is at gate and drain bias voltages fixed by regulators within the LNA. The bias voltages and currents at 25  $^{\circ}\text{C}$  are given in the caption of Fig. 3. The measured 1 dB gain compression power at 1.4 GHz is -24 dBm at input and +13.7 dBm at output.

Further confidence in the LNA model is shown in Fig. 6 which compares measured and modeled  $S$  parameters of the LNA at 27  $^{\circ}\text{C}$  as a function of frequency. The measured  $S_{12}$  is <-48 dB from 0.01 to 2 GHz.

The most important results of this paper are shown in Fig. 7 and 8 which depict the frequency and temperature dependence of the noise. The shape of the modeled and measured noise differs somewhat due to measurement error above 1.5 GHz (where the amplifier match is poor) and due to modeling error which did not include the electromagnetic modeling of the transition between the suspended substrate input transmission line and the bond-wire connection to the transistors gate pad. However, the important message in this data is the large variation of noise vs temperature independent of frequency.

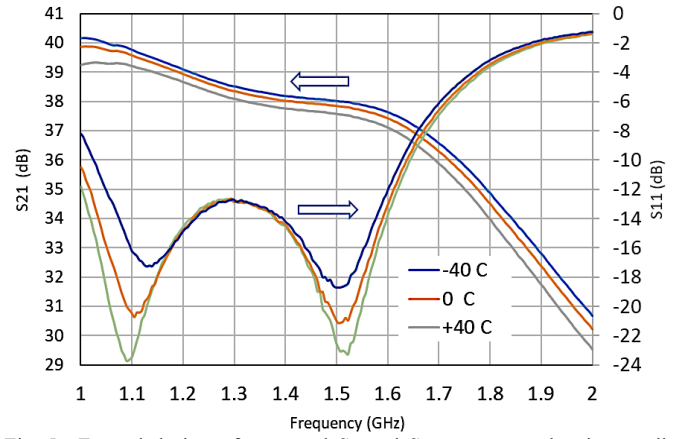


Fig. 5. Expanded view of measured  $S_{21}$  and  $S_{11}$  parameters showing small variation with temperature from -40  $^{\circ}\text{C}$  to +40  $^{\circ}\text{C}$ .

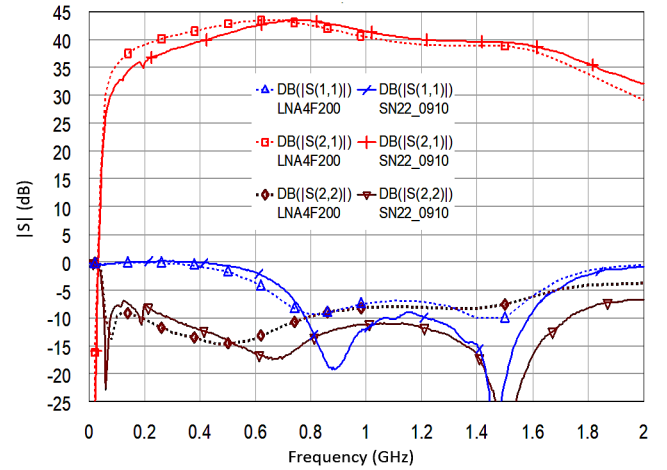


Fig. 6. Measured (solid lines) and modeled (dotted line)  $S$  parameters at 27  $^{\circ}\text{C}$ .

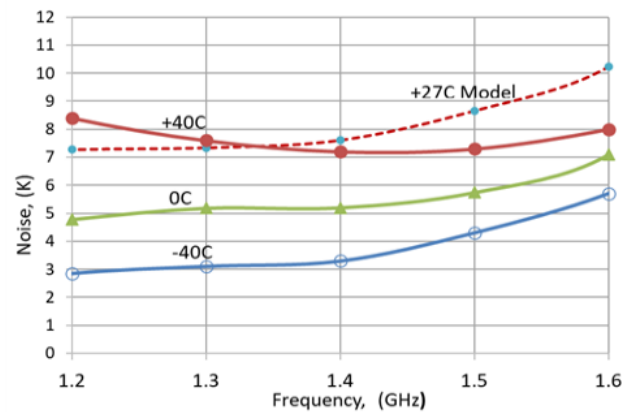


Fig. 7. Measured noise vs frequency at -40  $^{\circ}\text{C}$ , 0  $^{\circ}\text{C}$ , and +40  $^{\circ}\text{C}$ , and modeled noise at +40  $^{\circ}\text{C}$  for a typical LNA.

The linear component of decrease in noise shown in Fig. 8 would result in negative noise temperature below 127 K and thus there must be upward curvature at lower temperatures. Noise measurements of the LNA below 233 K are difficult because the voltage regulators in the bias circuit do not operate below -40  $^{\circ}\text{C}$  and the transistor is not properly heat sunk for cryogenic measurements. The bias problem was circumvented in a special test unit but the poor heat sinking caused errors due



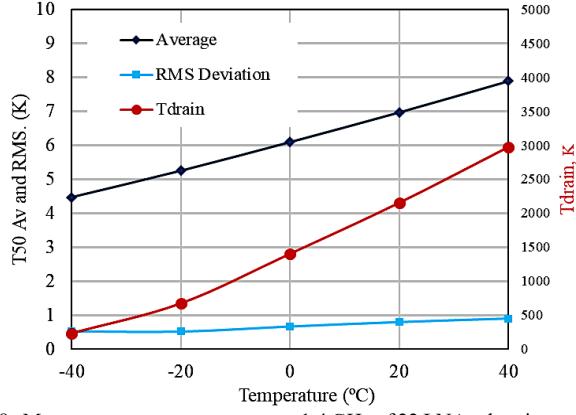


Fig. 8. Measurements vs temperature at 1.4 GHz of 22 LNAs showing average noise temperature,  $T_{50}$ , measured with 50  $\Omega$  source, rms deviation, and computed  $T_{\text{drain}}$  to give measured noise. Note that the  $S$  parameters shown in Fig. 4 change very little with temperature, and changes such as transconductance in the model are not the source of the noise variation with temperature.

to different thermal time constants in the vacuum cryocooler setup used for the measurements. The most believable result from these tests is a noise of  $2 \pm 1$  K at 120 K. Future investigations with better heat sinking and an optimum cryogenic noise matching circuit should result in even lower noise.

An important source of error in LNA noise vs temperature measurements is the noise due to the connecting cable between a cold LNA and the noise source-off termination at ambient temperature. For the data in this paper the connecting copper cable was 30 cm long with a loss of 0.22 dB which was entered into the noise figure analyzer as a pre-device-under-test attenuation at 300 K. This subtracts 15.5 K that can be validated with a measurement without the cable. However, the cooling of the end of the cable near the LNA at  $-40$  °C reduces the 15.5 K added noise by 1.0 K and thus must be added as a correction to the LNA noise indicated by the analyzer. This assumes 0.15 dB of the cable loss is at the average temperature of the two ends. This estimate not large compared to the measured 3.4 K noise reduction due to cooling of the LNA.

To dig deeper into the temperature behavior of the noise the AWR circuit simulator was utilized with the Pospieszalski noise model [4], [5] applied to the Diramics transistor [1] model shown in Fig. 4, and the remaining LNA circuit. This allows the sources of noise and their temperature dependence to be identified as shown in Table I. It is important to note that all resistances in the HEMT model represent thermal noise at ambient temperature except the drain-to-source resistance which is at a high temperature,  $T_{\text{drain}}$ , to represent the hot-electron noise. Thus, this one number and the ambient temperature,  $T_a$ , gives a complete noise model of the transistor including key quantities such as the minimum noise,  $T_{\text{min}}$ , and generator impedance,  $Z_{\text{opt}}$ , to achieve  $T_{\text{min}}$ .

The modeled noise is a combination of thermal noise in the input network (parameter `_TEMPK` in AWR), thermal noise in the input transistor ( $T_a$  in the transistor model), hot electron noise in the input transistor ( $T_d$  in the model), and second stage noise, all shown in Table I. These are all referred to a 50  $\Omega$  generator at the input. By superposition the noise components add to a total close to the measured total noise and do so because

TABLE I  
MEASURED AND MODELED NOISE AT  $-40$  °C TO  $+40$  °C

Quantity	$T_{\text{phys}}$ -40 °C	$T_{\text{phys}}$ 0 °C	$T_{\text{phys}}$ +40 °C
Measured total noise	4.5	6.1	7.9
Modeled thermal noise due to circuit loss	1.9	2.2	2.6
Modeled HEMT thermal noise	2.3	2.6	3.0
Modeled HEMT drain noise	0.4	1.0	2.4
Modeled second stage noise	0.2	0.2	0.2
Modeled total noise	4.8	6.0	8.2
$T_{\text{drain}}$ (K), to match measured total noise	233	973	2900

TABLE II  
NOISE PARAMETERS OF THE LNA AT  $+40$  °C

Freq. (GHz)	$T_{50}$ (K)	$T_{\text{min}}$ (K)	$R_{\text{opt}}$ ( $\Omega$ )	$X_{\text{opt}}$ ( $\Omega$ )	$R_N$ ( $\Omega$ )	$G_{\text{opt}}$ (S)	$G_{\text{opt}}$ $N=R_N$	$R_{\text{opt}}$ (K)
1.0	17.0	8.5	39.9	48.5	1.7	0.010	0.017	19.4
1.1	14.0	8.3	38.0	37.3	1.1	0.013	0.015	17.1
1.2	11.7	8.3	38.4	26.9	0.7	0.017	0.012	14.5
1.3	10.0	8.3	41.0	17.3	0.5	0.021	0.010	12.1
1.4	9.0	8.4	46.3	8.5	0.5	0.021	0.010	11.5
1.5	8.8	8.6	55.0	1.0	0.6	0.018	0.011	13.0
1.6	9.5	8.9	67.9	-3.5	0.9	0.015	0.013	15.6
1.7	11.0	9.3	84.9	-1.4	1.3	0.012	0.016	18.3
1.8	13.3	9.8	101.7	12.0	1.9	0.010	0.018	20.9
1.9	16.3	10.5	108.5	36.2	2.4	0.008	0.020	23.5
2.0	10.0	11.2	99.1	60.1	3.0	0.007	0.022	26.0

the drain noise temperature, also stated in the table, has been adjusted accordingly. It is surprising that  $T_{\text{drain}}$  is reduced by a factor of 12 for only a change of  $313/233 = 1.3$  in absolute temperature.

The complete noise model of the LNA allows the noise parameters to be computed as shown in Table II. The noise parameters allow the noise wave coming out of the input of the LNA to be calculated; a useful quantity for closely coupled feeds or antennas.

#### IV. SYSTEM PERFORMANCE

Two of the LNAs described in this paper have been installed on a radio telescope at the Caltech Radio Observatory near Bishop, CA. The telescope shown in Fig. 9 is part of the DSA110, a dual-linear polarized, 110-element radio telescope array requiring 220 LNAs. An expansion to DSA2000, a 2000-element, radio camera for the 0.7 to 2 GHz range [12] is being proposed.

An important criterion for the sensitivity of the array is the system noise temperature,  $T_{\text{sys}}$ , with components shown in Table III. With the LNA described in this paper, a  $T_{\text{sys}}$  of 22 K has been measured by the absorber vs sky Y factor method. The values for cosmic background, galactic, and atmospheric noise are known from many previous studies and with errors of the order of 1 K due to weather and direction of the antenna. The values for spillover, feed blockage, and feed loss are from extensive analysis of the feed using CST software and may vary by 2 K due to antenna elevation angle and soil moisture.

A previous version of the array utilized a more conventional LNA with a noise temperature of 32 K and  $T_{\text{sys}}$  of approximately 60 K. The 38 K improvement was due to 25 K from the LNA and 13 K due to reduction feed loss and spillover. This system temperature is comparable to that obtained in

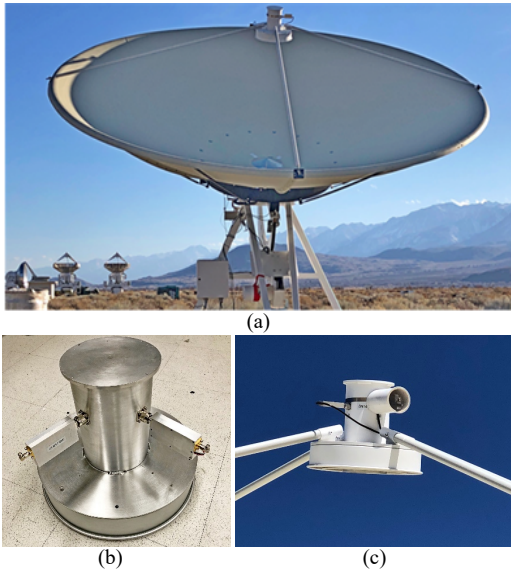


Fig. 9. (a) 4.6 m prime focus paraboloid, (b) LNAs mounted on low-loss, dual-linear polarization feed, and (c) feed mounted at prime focus of paraboloid.

TABLE III  
COMPOSITION OF MEASURED SYSTEM NOISE

Source	Noise (K)	Comment
Cosmic Background	2.7	Measured to mK accuracy in hundreds of experiments
Galactic	1	Spatial average of many discrete sources and will vary with location of galactic plane in antenna beam
Atmosphere	3	Oxygen and water at 30-degree zenith angle
Spillover	3	Calculated from feed pattern; higher at zenith
Feed Blockage	2	Estimate based upon 0.38 m feed diameter and 150 K average brightness of scattered pattern
Feed Loss	2	EM integration of surface current and surface resistance
$T_{\text{LNA}}$	7	Measure in laboratory with noise source calibrated with LN <sub>2</sub>
Post LNA Noise	1	Due to 600 K next stage, 3 dB cable loss, and 36 dB LNA gain + fiber link noise
Total	21.7	Total measured with absorber vs sky, Feb 20, 2020

cryogenic radio telescope systems such as the 100 m telescope at the Green Bank Observatory. [13].

#### V. NOISE CALIBRATION

Commercially available noise sources such as the Keysight N4000A have a stated ENR calibration uncertainty of  $\pm 0.16$  dB in the 0.01 to 1.5 GHz range [14]. This is adequate for measurement of noise figures in the dB range but not for the subject LNA with 0.10 dB NF. Expressed in noise temperature error, the uncertainty is  $\pm 11$  K. The noise temperatures reported in this paper have been measured with a N4000A noise source calibrated by 50  $\Omega$  terminations immersed in liquid nitrogen, LN<sub>2</sub>, near 77.4 K and near 300 K. The error in this type of calibration is limited by several factors which are discussed below. Taking these errors into account the accuracy of the noise measurements presented in this paper is estimated to be  $\pm 1$  K in the 1.3 to 1.5 GHz range.

The basic procedure for calibrating the ENR of a noise diode is to measure the noise out of an LNA with hot and cold thermal noise standards at its input. The same LNA is then measured

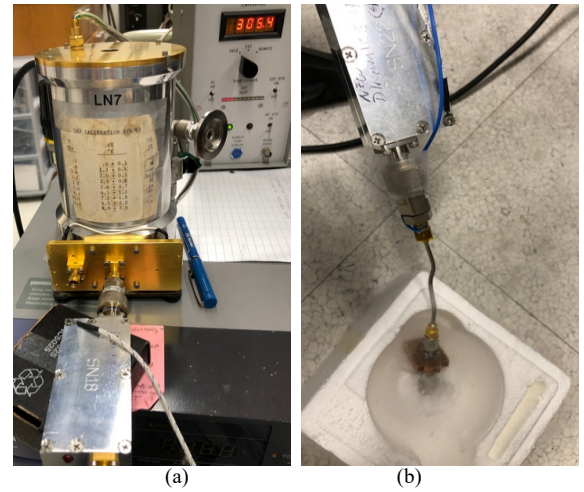


Fig. 10. Two methods of using LN<sub>2</sub> cooled terminations to measure the noise of an LNA and then calibrate noise diodes for faster measurements.

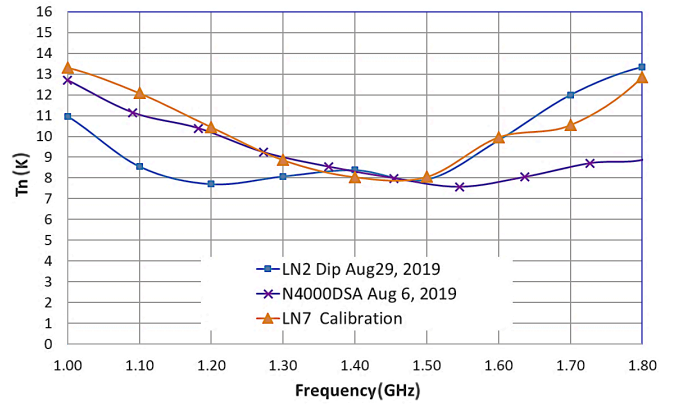


Fig. 11. Noise temperature measurements using the two methods of Fig. 10. There is good agreement in the design frequency range, 1.28 to 1.53 GHz of the current LNA.

with the diode noise source with ENR adjusted to give the same noise temperature. The cold termination is connected to the LNA through a coaxial line near 77 K at one end and near 300 K at the end connected to the LNA. The noise contribution of this coaxial line must be known and is computed from the dimensions and conductivity of the metals vs temperature as described in [15].

The calibration has been performed with two very different apparatus which are shown in Fig. 10 with results compared in Fig. 11. . The apparatus shown in Fig. 10 (a) is a small LN<sub>2</sub>-cooled vacuum dewar designed by one of the authors at National Radio Astronomy Observatory in 1987. The 50  $\Omega$  cold termination is thermally connected to the bottom of a spherical LN<sub>2</sub> tank in the vacuum chamber and also has a platinum-resistance temperature sensor attached to the termination. As a check the simple setup shown in Fig. 10 (b) has been used and consists of a rigid coaxial line with SS outer and BeCu inner conductor connected to a 50  $\Omega$  termination which can be dipped in LN<sub>2</sub>. The results of noise temperatures measured by both methods are compared om Fig. 11 with <1 K discrepancy between 1.3 and 1.5 GHz. In the 1 to 2 GHz band the peak discrepancy is approximately 3 K as discussed below.

The sources of error in the calibration are the following:

TABLE IV  
COMPARISON WITH PREVIOUS WORK  
All in coaxial enclosures with noise referred to input connector

Ref.	Temp. (K)	Freq. (GHz)	Noise (K)	$S_{21}$ (dB)	$S_{11}$ (dB)	DC Power (mW)	Tech.
This paper Fig. 4	313	1.4	7.5	38	-14	255	InP
	233	1.4	3.3	38	-14	255	InP
Schleeh [4]	300	1.0	10	50	-16	193	InP
G8FEK [18]	298	1.4	32	30	-10	1188	GaAs
MCL [16]	298	1.4	47	20	-17	204	GaAs
	228	1.4	27	21	-17	208	GaAs
Miteq [17]	296	1.4	34	32	-12	3000	GaAs
CMT [19]	23	1.0	3.5	35	-10	55	GaAs
LNF [20]	4	1.4	1.0	28	-10	6	InP

- 1) In Fig. 10, the termination in (a) is heat-sunk to the bottom of a small tank of LN<sub>2</sub> in the vacuum chamber but there is a thermal gradient between the termination temperature and the LN<sub>2</sub> temperature. A platinum resistance temperature sensor is closely attached to the termination and reads 80.4 K. For (b) the termination is in liquid LN<sub>2</sub> at 77.1 K for 200 m above sea level.
- 2) The cold terminations are connected to the LNA used for calibration by low-loss 3.58 mm diameter coaxial lines. In the case of (a) the loss of this line at 300 K is 0.055 dB and the noise at the LNA type N jack is calculated to be 83.7 K including the 0.025 dB loss of an SMA/N adaptor. For case (b) the line loss at 300 K is 0.13 dB and the noise at the LNA input jack is calculated to be 82 K.
- 3) The impedances of the cold and hot noise standards and of the noise diode in on and off states are close to 50  $\Omega$  with measured reflection coefficient of <-30 dB. However, the error due to the source mismatch depends on the  $S_{11}$  of the LNA shown in Fig. 4, which is of the order of -15 dB at in the 1.3 to 1.5 GHz range but just a few dB at 2 GHz. This causes errors which are as large as 3 K in the 1-2 GHz range and are difficult to correct. The most dominate error due to mismatch is the change in gain of the LNA between hot and cold terminations. To mitigate this error all measurements are made with the same termination for cold and hot with temperature changed by adding LN<sub>2</sub>.

## VI. SUMMARY AND CONCLUSIONS

The results of this paper compared to previous low noise amplifiers, both at ambient and cryogenic temperatures are shown in Table IV.

In conclusion the paper has presented the following unique or novel findings:

- 1) Table IV shows 4.2 times lower noise at 1.4 GHz compared to the best commercially available ambient-temperature LNAs we have found. This can have large impact on systems with low background noise such as utilized in space-to-ground communications, GPS location, or radio astronomy.
- 2) In Fig. 7, a large decrease in noise with cooling to -40 °C, an effect not predicted by existing HEMT noise theory and a challenge to further theoretical work.
- 3) In Table III, presentation of measured system noise with the LNA installed on an antenna; these results corroborate with laboratory tests.

- 4) Introduction of an internal noise calibration source for measurement of system noise.
- 5) In Table II, presentation of the modeled four noise parameters of the LNA; this is usually not included in LNA papers.
- 6) In section V, presentation of the noise source calibration using two different LN<sub>2</sub> noise standards.
- 7) Introduction of a design using a suspended-substrate transmission line bonded to a transistor die from a new InP HEMT foundry (Diramics).

The LNA is a first approach to “smart LNAs” which include multiplex circuitry for monitor and control utilizing tones on the output coaxial cable which also supplies DC bias. In the present case the internal noise calibration source is controlled by the detection or absence of a 32 kHz tone which is on when the calibration noise is desired. This tone is easily filtered from the DC bias and RF circuitry and is off during normal operation. It is suggested that future “smart LNAs” will include microprocessors and non-volatile memory for bi-directional control of functions such as input switching, frequency range, and gain along with monitoring of DC bias current, temperature, and log-RF output power.

## ACKNOWLEDGEMENT

Sander Weinreb and Jun Shi contributed equally to this work. We thank David Hodge and Hector Navarrete for much of the assembly work, Ralf Fluckiger for the excellent transistors, and Hamdi and Houssein Mani for suggestions and machining of the modules.

## REFERENCES

- [1] D. R. Williams, W. Lum, and S. Weinreb, "L-band cryogenically-cooled GaAs FET amplifier," *Mic. Jour.* 23 (1980): 73-76J.
- [2] D. Gallego and M. W. Pospieszalski, "Design and Performance of Cryogenically-Coolable Ultra Low Noise, L-Band Amplifier," *1990 20<sup>th</sup> Eur. Micr. Conf.*, Budapest, Hungary, 1990, pp. 1755-1760, doi: 10.1109/EUMA.1990.336325.
- [3] *Type pH-100 discrete InP HEMT*, Diramics AG, Zurich, Switzerland, <https://diramics.com/products/>.
- [4] J. Schleeh, N. Wadefalk, P. Å. Nilsson and J. Grahn, "10 K room temperature LNA for SKA band 1," *2016 IEEE MTT-S International Microwave Symposium (IMS)*, pp.1-4, 2016.
- [5] M. R. Murti et al., "Temperature-dependent small-signal and noise parameter measurements and modeling on InP HEMTs," *IEEE Trans. Microw. Theory Techn.*, vol. 48, no. 12, pp. 2579-2587, Dec. 2000.
- [6] P. Cheng, A. Y. Choi, and A. J. Minnich, "Microscopic mechanisms of hot electron noise can be calculated from first principles electron-phonon scattering", *APS March 2020 Meeting, Session H71.413*, Denver, CO, Mar.2-6, 2020.
- [7] A. Y. Choi, P. S. Cheng, and A. J. Minnich, "Electronic noise of warm electrons in semiconductors from first-principles," *arXiv:2009.11395v1*, 23 Sep 2020.
- [8] M. W. Pospieszalski, "Modeling of noise parameters of MESFETs and MODFETs and their frequency and temperature dependence," *IEEE Trans. Microw. Theory Techn.*, vol. 37, no. 9, pp. 1340-1350, Sept. 1989.
- [9] M. W. Pospieszalski, "Ultra-low-noise receivers for the 1 to 120 GHz frequency range," *1993 23rd European Microwave Conference*, Madrid, Spain, 1993, pp. 73-79.
- [10] *Microwave Noise in Semiconductor Devices*, H.L. Hartnagel, et al, Wiley, 2001, pp. 209-219.
- [11] *Reference Data for Engineers: Radio, Electronics, Computer, and Communications*, 7th ed., H. W. Sams, Indianapolis, IN, USA, 1985, p. 27-29 and 34-3.
- [12] G. Hallinan, et al, "The DSA-2000 – A Radio Survey Camera", *arXiv:1907.07648v1 [Astro-ph.IM]* 17 Jul 2019.



- [13] S. White, "Cm Receiver Design Considerations". *GBO Report*, <http://www.naic.edu/~astro/sdss5/talks/ReceiverSystem.pdf>.
- [14] *Keysight N4000 noise source., technical overview, 5988-0081. p. 8*, <https://www.keysight.com/us/>.
- [15] A. Soliman, A. Janzen, and S. Weinreb, "Thermal modelling of coaxial line for cryogenic noise measurements," *2016 URSI Asia-Pacific Radio Science Conference (URSI AP-RASC)*, Seoul, 2016, pp. 900-903.
- [16] *Data sheet, ZX60-P162LN+*, Mini-circuits, Inc, Brooklyn, NY, [www.minicircuits.com](http://www.minicircuits.com).
- [17] *Data sheet, LNA-30\_01000200-06-10P*, Narda-Miteq, Hauppauge, NY, [www.nardmiteq.com](http://www.nardmiteq.com).
- [18] *Model SBA 1300/1700*, RF Design, E. Yorkshire, UK, [www.g8FEK.com](http://www.g8FEK.com).
- [19] *Model CITLF3*, Cosmic Microwave Technology, Lawndale, CA, [www.cosmicmicrowavetechnology.com](http://www.cosmicmicrowavetechnology.com).
- [20] *Model LNF-LNCO.2-3*, LowNoiseFactory, Onsala, Sweden, [www.lownoisefactory.com](http://www.lownoisefactory.com).



**Jun Shi** (S'12-M'18) was born in Jiangsu Province, China, in 1988. He received the B.S. degree in information engineering and the Ph.D. degree in electromagnetic field and microwave technology from Southeast University, in 2011 and 2018, respectively. His Ph.D. dissertation was in the area of wideband feed technology and cryogenic receiver design technique applied to radio astronomy.

Since 2018, he is a Postdoctoral Scholar with the Microwave Research Group in the Department of Astronomy, California Institute of Technology, Pasadena, CA, USA. He has been a visiting student researcher at Caltech in the department of Electrical Engineering from 2015-2016. He has been a joint Ph.D. student in Shanghai Astronomical Observatory from 2013-2015. His current research interests include decade bandwidth antennas, ultra-low noise amplifiers, microwave circuit components, and RF systems.



**Sander Weinreb** (S'56-M'63-SM'71-F'78-LF'02) was born in New York, NY, on December 9, 1936. He received the BS and Ph.D. degrees in electrical engineering from MIT, Cambridge, Massachusetts, USA, in 1958 and 1963, respectively. He received the 1958 Boston Section IRE Award for Most Outstanding Electrical Engineering Senior at MIT. His Ph.D. dissertation was in the area of digital autocorrelation techniques applied to radio astronomy.

He presently is a Research Associate at Caltech in the department of astronomy. From 1999 to 2019 he has been a Faculty Associate at Caltech and a Principal Staff Member at Jet Propulsion Laboratory, Pasadena, CA where his major interest was large arrays for space communication and radio astronomy. From 1965-1983 he was Head of the Electronic Division ('65-'85) and Assistant Director ('86-'88) at National Radio Astronomy Observatory, Charlottesville, VA. He led the electronics design of the Very Large Array in New Mexico ('70-'76). He has been a visiting researcher or faculty member at U. of California Berkeley ('76-'78), U. of Virginia ('87-'89), and U. of Massachusetts - Amherst ('96-'99). During 1989-1996 he was Principal Scientist and Leader of the Millimeter Wave Design and Test Group at Martin Marietta Laboratories - Baltimore. He

is the author of over 150 publications in the areas of digital correlation techniques, radio astronomy observations, array receivers, and low noise mixers and amplifiers.

Dr. Weinreb was elected as an IEEE Fellow for "Contributions to Instrumentation in Radio Astronomy" and has served on many IEEE MTT technical committees and paper review teams. He was a 1985 MTT National Lecturer giving 35 presentations of "Radio Astronomy - A Challenge to the Microwave Engineer". He has served on advisory committees to several national and international radio observatories, was an advisor to the NASA Search for Extraterrestrial Life Program ('91-'97), and a US delegate to the Soviet Space Research Institute ('86-'87). He was nominated to the US Army Science Board ('91). He is a member of Commission J of URSI and was elected delegate to several international Meetings.